Gold coated optical fibers as three-dimensional electrodes for microfluidic enzymatic biofuel cells: Toward geometrically enhanced performance

Denis Desmaële,[1,a)] Louis Renaud,[2] and Sophie Tingry[1]
[1]*Institut Européen des Membranes, UMR 5635, ENSCM-UMII-CNRS, place Eugène Bataillon, 34095 Montpellier, France*
[2]*Université de Lyon, Institut des Nanotechnologies de Lyon INL-UMR5270, CNRS, Université Lyon 1, Villeurbanne F-69622, France*

(Received 13 July 2015; accepted 7 August 2015; published online 18 August 2015)

For the first time, we report on the preliminary evaluation of gold coated optical fibers (GCOFs) as three-dimensional (3D) electrodes for a membraneless glucose/O_2 enzymatic biofuel cell. Two off-the-shelf 125 μm diameter GCOFs were integrated into a 3D microfluidic chip fabricated via rapid prototyping. Using soluble enzymes and a 10 mM glucose solution flowing at an average velocity of 16 mm s^{-1} along 3 mm long GCOFs, the maximum power density reached $30.0 \pm 0.1\ \mu W\,cm^{-2}$ at a current density of $160.6 \pm 0.3\ \mu A\,cm^{-2}$. Bundles composed of multiple GCOFs could further enhance these first results while serving as substrates for enzyme immobilization. © *2015 AIP Publishing LLC*.
[http://dx.doi.org/10.1063/1.4928946]

I. INTRODUCTION

Laminar flow-based glucose fuel cells (LF-GFCs) are a subtype of microfluidic biofuel cells in which enzymes are used as biocatalysts to produce electrical energy from the oxidation of glucose coupled to the reduction of dioxygen. Considering their micrometer-sized fluidic channels, LF-GFCs can exploit the specific characteristics of the laminar regime. Particularly, in LF-GFCs, fuel and oxidant streams can flow side by side without significant convectional mixing.[1–3] Because only diffusion mixing is present, anode and cathode reactions can remain sufficiently separated so that no cross-over occurs. In the meantime, protons are still allowed to transport across the fluid-fluid interface. Consequently, and unlike conventional fuel cells, LF-GFCs eliminate the need for a proton exchange membrane to separate the anodic and cathodic compartments. This simplifies their miniaturization while reducing fabrication costs. Therefore, LF-GFCs appear as ideal candidates to develop miniature power sources for low consumption electronic systems.[4,5] Nonetheless, it is still needed to improve the performance of LF-GFCs. In this perspective, three-dimensional (3D) electrodes are promising. Indeed, microtextured 3D electrodes have the potential to enhance mass transfer of fresh reactants to the reactive electrode surface.[6] Moreover, 3D electrodes can increase the enzyme loading by offering enlarged reactive surface areas.[7] Several types of 3D electrode architectures such as herringbone ridges,[6] graphite rods,[8] or flow-through porous electrodes[9] were evaluated in membraneless laminar fuel cells that used various chemical reactants. Most of their enzymatic counterparts, however, solely used conventional planar electrodes.[10–14] Compared to such 2D electrodes, gold coated optical fibers (GCOFs) can offer distinct advantages: (i) meters of fibers already covered by a layer of gold are commercially available at an affordable price (≈ 1€ cm^{-1}); (ii) neither advanced microfabrication process nor access to a clean room is required for their integration in LF-GFCs; (iii) the gold area exposed to the reactants can be tuned without the need to

a)denis.desmaele@musciences.com

fabricate a new fluidic chip. In this work, we hence propose to evaluate GCOFs as 3D electrodes for a LF-GFC.

II. EXPERIMENTS

For preliminary tests, we ordered 3 m of a GCOF having an outer diameter (OD) of 125 μm (AFS 125G, AMS Technologies). From the fiber sample received, two 5 cm long GCOFs were cut using a scalpel. Because we did not intend to exploit the optical properties of the fibers, their extremities were not properly cleaved. The fibers were then cleaned with ethanol and rinsed with deionized water. Interconnecting optical fibers with microfluidic devices can be delicate and time-consuming.[15] For an easy implementation of the two GCOFs within a LF-GFC, we fabricated a specific 3D microfluidic chip made of networked circular microchannels. The fabrication method was adapted from previous protocols[16,17] to suit our specific purpose. It involved neither costly equipment nor the need to access to a clean room. In our case, we assembled manually a mold constituted of syringe needles (Neolus 0.8 $\times$ 40 mm, Terumo). Needles were cut and their extremities were polished using a precision grinding tool (Micromot 50/E, Prooxon). Two needles were aligned side by side with the aim of obtaining a central microchannel whose shape is similar to two intersecting circles (i.e., the main channel has a *binocular-like* cross-section). Two shorter needles were placed in a Y-shape to form the inlets. After control of the overall structure alignment, small pieces of candle wax were deposited between needle junctions using tweezers. Subsequently, gaps between needle connections were filled via capillarity by melting the wax pieces using a lighter (see Fig. 1(a)). The Y-shaped assembly of branched needles was then cautiously positioned on top of two pre-cured Polydimethylsiloxane (PDMS) slabs were placed in a Petri dish (see Fig. 1(b)). The remaining

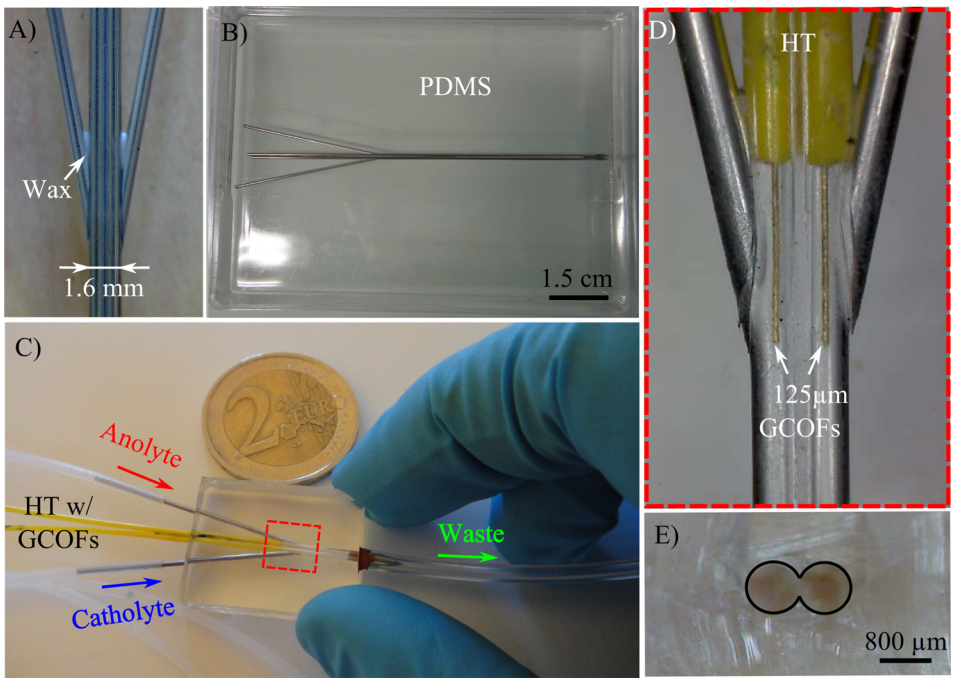

FIG. 1. (a) Picture illustrating the mold assembly process for fabricating the 3D LF-GFC developed in this work. Syringe needles are manually aligned and temporarily attached using small pieces of candle wax that are heated to fill gaps at needle junctions via capillary effects. (b) The entire mold of networked needles is placed on top of cured PDMS slabs inside a Petri dish for replication. Liquid PDMS is poured and allowed to cure according to common soft-lithography procedures (see text for details about all subsequent steps). (c) Overview of the final 3D LF-GFC obtained. The area indicated by red dashed lines is enlarged in Fig. 1(d). The diameter of the 2€ coin is 25 mm. (d) Magnified view showing 3 mm long GCOFs centered within each side of the main microchannel. The gold surface of each fiber is 1.2×10^{-2} cm^2. (e) Optical micrograph of a PDMS slice showing the *binocular-like* shape of the main microchannel cross section (edges are circled in black for better viewing).

of the fabrication process is inspired by standard soft-lithography procedures.[18] Briefly, a liquid mixture of PDMS was prepared in a 1:10 ratio of curing agent and PDMS monomer. It was degassed using a desiccator to remove air bubbles and poured over the needle mold. PDMS was then cured at 70 °C during 1 h. Sides of the cured PDMS were cut with a razor blade and the PDMS replica was immersed in acetone to make the PDMS channels slightly swell. Needles entrapped were then gently pulled out using pliers. Residues of melted wax were dissolved by flushing acetone into the channels with a syringe. After trimming, hytrel tubing (HT) having an inner diameter of 125 μm and an OD of 900 μm (FT900SM, Thorlabs) was inserted into the chip. New cut needles coupled to Polytetrafluoroethylene (PTFE) tubes were placed for the delivery and removal of fluids (see Fig. 1(c)). Silicone paste (JS 53, Loctite) was deposited to prevent leakage. Finally, the GCOFs were introduced into the HT. Considering its dimensions, the HT allowed a proper alignment so that the GCOFs were automatically centered within each side of the channels (see Fig. 1(d)). The length of the GCOFs to be in contact with the reactants was accurately set using an USB microscope (Discovery VMS-001, Veho). In this work, the lengths of the anode fiber and the cathode fiber were always equal, and the interspace between them was 800 μm. After setting, some candle wax was placed at the extremity of the HT positioned outside the fluidic chip. The position of the GCOFs was then temporarily maintained by melting the wax using an iron solder. During experiments, the pieces of wax could be removed so that the length of the GCOFs could be modified.

Glucose and oxygen solutions were prepared according to protocols reported elsewhere.[11,19] Briefly, glucose is oxidized to generate gluconolactone at the anode, whereas oxygen is reduced to water at the cathode. Enzymatic reactions occur via the use of glucose oxidase from *Aspergillus niger* (1 mg ml^{-1}, 198 000 U mg^{-1} solid) and hexacyanoferrate (10 mM) flowing in the anolyte solution, whereas freely suspended 2,2′-azino-bis(3-ethylbenzothiazoline-6-sulfonic acid) diammonium salt (ABTS) (1 mg mL^{-1}) and laccase from *Trametes versicolor* (1 mg mL^{-1}, 20 U mg^{-1} solid) are introduced in the catholyte stream. Solutions were then transferred in 10 ml capacity syringes (BD Discardit II) and injected into the fluidic chip using a syringe pump (KDS200, KD Scientific). The flow rate imposed by the syringe pump was set to 500 μl min^{-1}. This specific flow rate was selected to obtain an average flow velocity of $\approx$16 mm s^{-1} so that a comparison with 2D gold electrodes previously reported[10] could be facilitated. Measurements were conducted at room temperature ($\approx$20 °C) using a potentiostat (Autolab, Eco chemie). Electrode leads were attached to each GCOF using alligator clips. The working electrode of the potentiostat was connected to the cathode fiber, whereas both the counter and reference electrodes of the potentiostat were connected to the anode fiber.

Tests were first conducted using 8 mm long GCOFs. Fig. 2(a) shows the polarization curve obtained (solid line with squares). With no current flowing through an external load, the average open circuit voltage (OCV) is 0.39 $\pm$ 0.1 V. The polarization curve then behaves according to the I-V profiles observed for conventional fuel cells.[20] Notably, as the current is increased, there is a region almost linear ($\approx 1 < I < 3$ μA) where ohmic losses lower the voltage. At a certain point ($I \geq 3.5$ μA), the voltage drops more abruptly because mass-transfer limitations become predominant. These losses are due to the fact that reactants are not being able to reach the electrode surfaces.[21] At zero voltage, the short circuit current (ISC) is around 4.5 μA, whereas the maximum amount of net power produced is 635 nW at $\approx$0.19 V (see Fig. 2(b)). For comparison purposes, experiments were also carried out using 3 mm long GCOFs. Because these shorter electrodes had a reduced active area exposed to the reactants, the ohmic region is lowered and the ISC drops to $\approx$3 μA (dashed line with circles, Fig. 2(a)). As expected, Fig. 2(b) also confirms that the amount of net power produced is significantly reduced when using shorter electrodes. Nonetheless, both the current density and the power density are enhanced when using shorter GCOFs. This is demonstrated in Figs. 2(c) and 2(d), where values are normalized according to the geometrical area of the GCOFs. When using 8 mm long GCOFs, the maximum power density is 20.2 $\pm$ 0.1 μW cm^{-2} at a current density of 107.4 $\pm$ 0.2 μA cm^{-2}. Comparatively, when using 3 mm long GCOFs, the maximum power density is increased by $\approx$50% and reaches 30.0 $\pm$ 0.1 μW cm^{-2} at a current density of 160.6 $\pm$ 0.3 μA cm^{-2}. Such trends are actually in accordance with results reported previously for planar gold electrodes.[22,23] As for

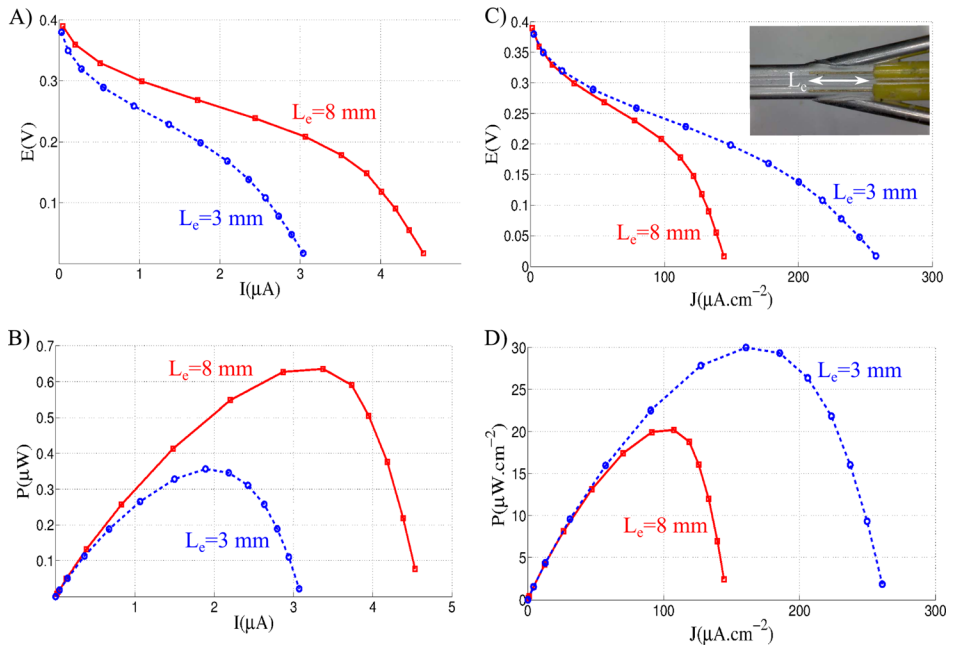

FIG. 2. Performance measured for the 3D LF-GFC fabricated. L_e represents the length of both GCOFs (i.e., the anode and cathode are equal in length). Solid lines with squares and dashed lines with circles correspond to results obtained using 8 mm long and 3 mm long GCOFs, respectively. (a) Polarization curves. (b) Power-current profiles. (c) Evolution of the voltage as function of the current density. (d) Power density as a function of the current density.

2D electrodes, it is indeed likely that thicker depletion layers develop along longer GCOFs and restrict their performance.[6,10,24] The most straightforward way to reduce the effect of depletion layers is to increase the flow rate. Nevertheless, we did not try to further increase the reference flow rate as in one of our former work[23] because we wanted to minimize reactants consumption. Additionally, it is likely that the overall performance of our present system is cathode limited.[25] Nonetheless, since our approach allows to tune the lengths of the anode and cathode independently, an extensive parametric study could be conducted to find the optimal anode/cathode ratio.[26] In any event, the maximum power achieved using 3 mm long GCOFs appears to be ≈20% higher than for 2D electrodes offering the same reactive surface under the same average flow velocity.[10] Although it remains delicate to straightforwardly compare the activity of the enzymes used in both configurations, it is presently assumed that the corners and sharp edges located at the GCOFs extremities have a positive effect on the overall performance of our LF-GFC.[27–30] Because the immobilization of enzymes on optical fibers has been demonstrated[31] and considering the possibility to readily group several fibers in compact bundles,[32,33] we believe that the use of GCOFs could pave the way for further improvements in the field of microfluidic LF-GFCs.

III. CONCLUSION AND FUTURE WORK

We have proposed a preliminary evaluation of commercial gold coated optical fibers as 3D electrodes for a membraneless laminar microfluidic biofuel cell. Via the fabrication of an original 3D microfluidic chip offering a *binocular-like* cross section, we integrated 3 mm long fibers with a volume of only $37 \times 10^{-6}\,\mathrm{cm}^3$ that offered a gold surface of $1.2 \times 10^{-2}\,\mathrm{cm}^2$. At room temperature, the maximum current density obtained was $160.6 \pm 0.3\,\mu\mathrm{A\,cm}^{-2}$ at 0.19 V, representing a maximum power density of $30.0 \pm 0.1\,\mu\mathrm{W\,cm}^{-2}$. Although these first results conducted with soluble enzymes and a 10 mM glucose solution are encouraging, there is still room for improvements. In the near future, we will seek to improve the performance of our configuration by using several fibers grouped in compact bundles. In particular, we will investigate the possibility to adapt a protocol previously published to immobilize enzymes on such fiber bundles via the encapsulation of carbon nanomaterials in polymer matrices.[34] Because several

studies reported performance alterations due to electrode stability problems,[35,36] we also plan to assess the stability of the GCOFs by conducting experiments over long periods of time. Finally, we envision that the optical properties of GCOFs might be exploited to add novel functionalities to membraneless biofuel cells.

ACKNOWLEDGMENTS

This work was supported by the ANR program "International II" under project "Hybiocell."

[1]R. Ferrigno, A. D. Stroock, T. D. Clark, M. Mayer, and G. M. Whitesides, J. Am. Chem. Soc. **124**, 12930 (2002).
[2]M. Sun, G. V. Casquillas, S. Guo, J. Shi, H. Ji, Q. Ouyang, and Y. Chen, Microelectron. Eng. **84**, 1182 (2007).
[3]J. wook Lee and E. Kjeang, Biomicrofluidics **4**, 041301 (2010).
[4]S. C. Barton, J. Gallaway, and P. Atanassov, Chem. Rev. **104**, 4867 (2004).
[5]W. Gellett, M. Kesmez, J. Schumacher, N. Akers, and S. D. Minteer, Electroanalysis **22**, 727 (2010).
[6]S. K. Yoon, G. W. Fichtl, and P. J. Kenis, Lab Chip **6**, 1516 (2006).
[7]V. Flexer, N. Brun, O. Courjean, R. Backov, and N. Mano, Energy Environ. Sci. **4**, 2097 (2011).
[8]E. Kjeang, J. McKechnie, D. Sinton, and N. Djilali, J. Power Sources **168**, 379 (2007).
[9]E. Kjeang, R. Michel, D. A. Harrington, N. Djilali, and D. Sinton, J. Am. Chem. Soc. **130**, 4000 (2008).
[10]K. G. Lim and G. T. R. Palmore, Biosens. Bioelectron. **22**, 941 (2007).
[11]A. Zebda, L. Renaud, M. Cretin, C. Innocent, R. Ferrigno, and S. Tingry, Sens. Actuators, B **149**, 44 (2010).
[12]T. Miyake, M. Oike, S. Yoshino, Y. Yatagawa, K. Haneda, and M. Nishizawa, Lab Chip **10**, 2574 (2010).
[13]T. Beneyton, I. P. M. Wijaya, C. B. Salem, A. Griffiths, and V. Taly, Chem. Commun. **49**, 1094 (2013).
[14]L. Renaud, D. Selloum, and S. Tingry, Microfluid. Nanofluid. **18**, 1407 (2015).
[15]D. M. Hartmann, J. T. Nevill, K. I. Pettigrew, G. Votaw, P.-J. Kung, and H. C. Crenshaw, Lab Chip **8**, 609 (2008).
[16]See http://blogs.rsc.org/chipsandtips/2010/05/03/rapid-prototyping-of-branched-microfluidics-in-pdms-using-capillaries/ for S. Ghorbanian, M. A. Qasaimeh, and D. Juncker, Lab Chip (2010).
[17]P. R. Hunziker, M. P. Wolf, X. Wang, B. Zhang, S. Marsch, and G. B. Salieb-Beugelaar, J. Micromech. Microeng. **25**, 025018 (2015).
[18]Y. Xia and G. M. Whitesides, Annu. Rev. Mater. Sci. **28**, 153 (1998).
[19]A. Zebda, L. Renaud, M. Cretin, F. Pichot, C. Innocent, R. Ferrigno, and S. Tingry, Electrochem Commun. **11**, 592 (2009).
[20]A. Z. Weber and J. Newman, Chem. Rev. **104**, 4679 (2004).
[21]J. B. Benziger, M. B. Satterfield, W. H. Hogarth, J. P. Nehlsen, and I. G. Kevrekidis, J. Power Sources **155**, 272 (2006).
[22]J. Lee, K. G. Lim, G. T. R. Palmore, and A. Tripathi, Anal. Chem. **79**, 7301 (2007).
[23]A. Zebda, L. Renaud, M. Cretin, C. Innocent, F. Pichot, R. Ferrigno, and S. Tingry, J. Power Sources **193**, 602 (2009).
[24]W. A. Braff, C. R. Buie, and M. Z. Bazant, J. Electrochem. Soc. **160**, A2056 (2013).
[25]A. Bedekar, J. Feng, S. Krishnamoorthy, K. Lim, G. Palmore, and S. Sundaram, Chem. Eng. Commun. **195**, 256 (2007).
[26]N. Uría, D. Sánchez, R. Mas, O. Sánchez, F. X. Munoz, and J. Mas, Sens. Actuators, B **170**, 88 (2012).
[27]Y. Wang, T.-C. Chang, P. R. Stoddart, and H.-C. Chang, Biomicrofluidics **8**, 021101 (2014).
[28]S. Basuray, S. Senapati, A. Aijian, A. R. Mahon, and H.-C. Chang, ACS Nano **3**, 1823 (2009).
[29]S. K. Thamida and H.-C. Chang, Phys. Fluids **14**, 4315 (2002).
[30]R. Zhou, P. Wang, and H.-C. Chang *et al.*, Electrophoresis **27**, 1376 (2006).
[31]T.-Q. Lin, Y.-L. Lu, and C.-C. Hsu, Opt. Express **18**, 27560 (2010).
[32]T. A. Dickinson, J. White, J. S. Kauer, and D. R. Walt, Nature **382**, 697 (1996).
[33]S. Szunerits and D. R. Walt, ChemPhysChem **4**, 186 (2003).
[34]D. Selloum, S. Tingry, V. Techer, L. Renaud, C. Innocent, and A. Zouaoui, J. Power Sources **269**, 834 (2014).
[35]M. J. González-Guerrero, J. P. Esquivel, D. Sánchez-Molas, P. Godignon, F. X. Muñoz, F. J. del Campo, F. Giroud, S. D. Minteer, and N. Sabaté, Lab Chip **13**, 2972 (2013).
[36]D. Desmaële, L. Renaud, and S. Tingry, Sens. Actuators, B **220**, 583 (2015).